A major purpose of the Technical Information Center is to provide the broadest dissemination possible of information contained in DOE's Research and Development Reports to business, industry, the academic community, and federal, state and local governments.

Although a small portion of this report is not reproducible, it is being made available to expedite the availability of information on the research discussed herein.

LA-UR -86-3695

Los Alamos National Laboratory is operated by the University of California for the United States Department of Energy under contract W-7405-ENG-36

LA-UR--86-3695

DE87 001988

TITLE TRAC-PF1/MOD1 PRETEST PREDICTIONS OF MIST EXPERIMENTS

AUTHOR(S) B. E. Boyack, J. L. Steiner, and D. A. Siebe

SUBMITTED TO Fourteenth Water Reactor Safety Information Meeting
October 27-31, 1986
National Bureau of Standards (NBS)
Gaithersburg, MD

DISCLAIMER

Los Alamos National Laboratory
Los Alamos, New Mexico 87545

TRAC-PF1/MOD1 PRETEST PREDICTIONS OF MIST EXPERIMENTS*

by

B. E. Boyack, J. L. Steiner, and D. A. Siebe

Safety Code Development Group
Energy Division
Los Alamos National Laboratory
Los Alamos, New Mexico 87545

ABSTRACT

Los Alamos National Laboratory is a participant in the Integral System Test (IST) program initiated in June 1983 to provide integral system test data on specific issues and phenomena relevant to post small-break loss-of-coolant accidents (SBLOCAs) in Babcock & Wilcox plant designs. The Multi-Loop Integral System Test (MIST) facility is the largest single component in the IST program. During Fiscal Year 1986, Los Alamos performed five MIST pretest analyses. The five experiments were chosen on the basis of their potential either to approach the facility limits or to challenge the predictive capability of the TRAC-PF1/MOD1 code. Three SBLOCA tests were examined which included nominal test conditions, throttled auxiliary feedwater and asymmetric steam-generator cooldown, and reduced high-pressure-injection (HPI) capacity, respectively. Also analyzed were two "feed-and-bleed" cooling tests with reduced HPI and delayed HPI initiation. Results of the tests showed that the MIST facility limits would not be approached in the five tests considered. Early comparisons with preliminary test data indicate that the TRAC-PF1/MOD1 code is correctly calculating the dominant phenomena occurring in the MIST facility during the tests. Posttest analyses are planned to provide a quantitative assessment of the code's ability to predict MIST transients.

INTRODUCTION

Los Alamos is currently providing analytical support to the Integral System Test (IST) program; the largest part of our analytical efforts involves the use of the TRAC-PF1/MOD1 code. TRAC is, or will be, used as a complement to the Multi-Loop Integral System Test (MIST) experimental program in three applications. The first of these is related to test specification or design. This assumes that one has sufficient confidence that TRAC will correctly predict the dominant test phenomena and, therefore, that the predicted results can be used to ensure that facility limits will not be exceeded and that the resultant test will satisfy the test objectives. For example, TRAC can be used to determine whether the design limits of the facility or facility instrumentation ranges could be exceeded during a test. The

* Work performed under the auspices of the US Nuclear Regulatory Commission.

second application is related to test evaluation. It is impossible to include all the desired instrumentation in a facility because of constraints such as cost, complexity, and space. Again, if one has sufficient confidence that TRAC will correctly predict the dominant test phenomena, calculations can be used to fill in gaps about quantities that are not measured in the facility. The third application is related to TRAC assessment. The ability of a thermal-hydraulic code to accurately calculate experimental behavior in scaled facilities is an important link in demonstrating that the code can be used to predict how an operating pressurized water reactor (PWR) would perform under accident conditions.

During Fiscal Year 1986, Los Alamos performed five MIST pretest analyses. The five experiments were chosen on the basis of their potential either to approach the facility limits or to challenge the predictive capability of the TRAC code. The five tests are identified and briefly discussed in the following paragraphs.

Test 310000. MIST test 310000 was the proposed nominal test for the MIST program. During the early test program, several repeats of this test were run. The test selected for the nominal, Test 3109AA, differs from the pretest specification for 310000 in the initial pressurizer liquid level and in efforts to warm the surge line and maintain the pressurizer liquid at saturation until test initiation. Thus, the TRAC pretest calculation was made for conditions slightly different from those in the selected nominal Test 3109AA. The nominal conditions include a scaled 10-cm^2 cold-leg (CL) discharge leak, full high-pressure injection (HPI) and auxiliary feedwater (AFW), unavailable reactor-coolant pumps (RCPs), no noncondensable gas injection, automatic reactor vessel vent-valve (RVVV) actuation on differential pressure, automatic guard heater control, constant steam generator (SG) secondary level control after SG refill, and symmetric SG cooldown.

Test 310503. This test focuses on the effect of throttled AFW and asymmetric SG cooldown. The longer-duration SG refill obtained by reducing the SG-refill rate is intended to obtain AFW boiler-condenser mode (BCM) cooling. Following SG refill, the SGs are to be depressurized at unequal rates, to generate asymmetric loop conditions. The purpose is to accentuate interloop asymmetries to investigate their long-term impact.

Test 320604. The tests of group 32 are controlled in the same manner as the Nominal Test (310000) but with altered leak and HPI characteristics. This test uses the Evaluation Model (EM) HPI capacity, which is roughly one-half that of full HPI. Relative to the nominal case, extensive system voiding and perhaps an early occurrence of the BCM are expected.

Test 330201. The tests of group 33 examine system interactions that occur while using feed-and-bleed (HPI - PORV) cooling. These tests simulate a total loss of secondary-side feedwater. Test 330201 uses the EM rather than the full HPI head-flow characteristics. EM HPI flow is initiated upon lifting of the power-operated relief valve (PORV).

Test 330302. This test imposes delayed HPI activation. The PORV discharge will be the only available energy-removal mechanism for the first 20 minutes following PORV lift. The full HPI is then provided.

Each of the five experiments described above has now been run in the MIST facility. Formal test reports and the data tapes are not currently available. However, limited results from several of the tests are available and can be used for qualitative assessment of TRAC's ability to predict the dominant phenomena in the tests. We will include a brief discussion, where test results are available.

CODE VERSION

We used an updated version 12.7 of the TRAC-PF1/MOD1 code (Ref. 1). The TRAC-PF1/MOD1 code was developed at Los Alamos National Laboratory to provide advanced best-estimate predictions of postulated accidents in light-water reactors. The code features a two-phase, two-fluid nonequilibrium hydrodynamics model with a noncondensable gas field; flow-regime-dependent constitutive equation treatment; either one- or three-dimensional treatment of the reactor vessel; complete control-systems modeling capability; a turbine component model; and a generalized steam-generator component model.

PLANT MODEL

Figure 1 is a MIST facility arrangement drawing. Figures 2 and 3 provide an overview of the TRAC MIST facility model. The TRAC model of the MIST facility has evolved over a period of time. The model was initially based on preliminary information provided in the MIST Facility Specification. It has progressed to its present form as available as-built facility information was received from Babcock & Wilcox (B&W). The model consists of 77 components that have been subdivided into 276 fluid cells. Only one-dimensional components are used in this model. The model is considered to be rather finely noded and is expected to predict the dominant phenomena during MIST experiments.

CALCULATION RESULTS

During analysis of our pretest calculations, we found that many of the predicted phenomena occurred in each of the calculations. Therefore, we have chosen to provide a detailed description of the nominal MIST Test 310000 and will provide less detailed descriptions for the remainder of the pretest predictions. The discussion in these cases will focus on the important phenomena that differ from those in the nominal case. We note that for each test calculation, at time zero, the primary was liquid full and coolant was being driven by natural circulation.

Test 310000. The transient calculation was started at time zero by the initiation of a scaled 10 cm^2 break just downstream of the HPI nozzle in the B1 cold leg (Fig. 1). As the pressurizer level fell below 0.3048 m (1 ft.)(at 45 s), several actions were taken. The core power ramp was started, HPI began, RVVV automatic control was initiated, and the RVVVs first opened.

Primary-system saturation first occurred at 80 s in the intact-loop hot leg (Fig. 4) as a result of the effects of the pressurizer liquid entering that leg. Natural circulation in the intact loop ended at 160 s (Fig. 5) when the hot-leg U-bend fully voided. This effectively decoupled the intact-loop SG as a heat sink. The broken-loop (B) hot leg first saturated at 110 s, for about 40 s duration. During this time, the void fraction remained small and there was little effect on the loop natural circulation. At about 420 s, the broken loop again saturated. This time flow through the loop declined rapidly until about 530 s, when the loop temporarily stalled. The declining primary-to-secondary heat transfer, caused by the decline in broken-loop flow, led to a temperature increase at the core exit beginning at about 440 s. The core exit liquid saturated at 500 s with the increasing temperature. This caused the system to begin repressurization (Fig. 6). As the broken loop stalled at 530 s, voiding in the reactor vessel upper head forced more liquid into the hot legs, immediately restarting flow through the broken-loop. This continued until 860 s when the U-bend voided completely and

the loop again stalled. The increased primary-to-secondary heat transfer from the renewed flow through the hot leg, along with leak-HPI cooling and the declining core power, caused the system to begin depressurizing again at about 725 s. An intraloop natural circulation started in the broken-loop cold legs just after circulation through the loop ended (Fig. 7). This flow goes from the downcomer, backwards through the broken cold leg, and forward through the other broken-loop cold leg.

Steam generator secondary depressurization is automatically controlled to a set point based on abnormal transient operator guidelines (ATOG) determined from core-exit temperature and the saturation temperatures corresponding to SG secondary pressures. Depending on these three temperatures, the ATOG-based set point pressure may be: (1) held constant, (2) reduced by 50 psi/min, or (3) reduced such that the corresponding saturation temperature is reduced by 100°F/h. Following reactor trip at 45 s, the SG control system received a signal to fill the secondaries to the 9.63 m (95%) level. The secondary-side collapsed liquid levels of the intact-loop and broken-loop SGs reached this level at about 500 and 540 s, respectively. During the refilling of the secondaries by the AFW, the secondary pressures were reduced (Fig. 6). In the intact loop, the secondary pressure remained below the ATOG-based set point pressure, resulting in termination of steam flow by the control system. Therefore, with the exception of a small flow as the control system settled in on the level set point, there was no supply of AFW to the intact-loop secondary after 500 s until the ATOG-based set point decreased to the intact-loop SG pressure at 3500 s. The broken-loop secondary pressure remained below the ATOG-based set point until 760 s. The controller is designed to allow steaming of the broken-loop SG secondary to maintain the set point pressure and provide AFW flow to maintain the liquid level; BCM heat transfer can occur when the primary liquid in the SG drops below the upper tube sheet and there is AFW flow. An event of this type occurred at about 2600 s and increased the rate of primary depressurization (Fig. 6). At 3500 s, when the ATOG-based set point reached the intact-loop SG secondary pressure, allowing steaming and AFW flow, the liquid level in the primary side was well below the tube sheet. This created a strong BCM event that increased the primary depressurization rate significantly (Fig. 6).

Refill started at about 3600 s when two-phase flow out the break started and HPI flow exceeded break flow (Fig. 8). It is expected that the break and HPI flows will have nearly the same magnitude for some time, with break flow gradually decreasing and HPI gradually increasing as the system depressurizes. The calculation was run to 3696 s, which is near the start of this phase. System liquid inventory should then gradually increase.

During nominal Test 3109AA, the following phenomena were observed: (1) interruption of natural circulation in the intact loop with continued intermittent natural circulation in the broken loop before complete interruption of circulation; (2) strong loop asymmetries in the hot-leg liquid levels and temperatures and in the cold-leg flow rates and temperatures; (3) weak SG performance without liquid flow through the loops resulting from BCM heat transfer and condensation in the SG primary side; and (4) intraloop natural circulation with flow from the downcomer, backward through one cold leg and forward through the adjacent cold leg. Each of these phenomena was predicted by TRAC. We note that there were significant quantitative differences between the predicted transient and the selected nominal Test 3109AA. However, the MIST facility has proven to be a very sensitive facility with strong coupling within the primary system and from the primary to the secondary system. A true quantification of

TRAC's ability to predict the MIST test must await posttest assessment efforts using the initial and boundary conditions measured during the test.

Test 310503. As in MIST Test 3109AA, the nominal test, the transient calculation was started at time zero by the initiation of a scaled 10-cm^2 break in the B1 cold leg just downstream from the HPI nozzle. The same initial control actions were taken for Test 310503 as for Test 310000, except that the SG refill rate was reduced. This was intended to alter the primary-to-secondary heat-transfer rates during SG refill by increasing the possibility for BCM heat transfer, and to change the system interactions. Later in the transient, asymmetric SG cooldown, with the SG depressurization rates controlled to decrease the intact-loop SG secondary saturation temperature by 100°F/h and the broken-loop secondary by 50°F/h, was used. The test was expected to provide data on the effect of accentuated asymmetries between the loops.

Many of the phenomena seen before the SGs refill to the set points that signal the beginning of controlled SG-secondary depressurization were similar to the phenomena predicted for the nominal transient. The primary-to-secondary heat transfer predicted was less for this case, which had a reduced SG-secondary refill rate, than for the proposed nominal case, Test 310000. Consequently, the depressurization rate was initially slower (Fig. 9) and the leak flow was higher. The interruptions of the loop flows are very similar to the interruptions seen in the nominal case, although the loop flows (Fig. 10) were smaller and these events occurred at different times. The intact loop saturated, the U-bend voided, and the loop stalled in a slightly longer time than calculated for specified Test 310000. This happened because the smaller primary-to-secondary heat transfer resulted in a slower depressurization rate and initial saturation was not reached as quickly. The broken loop continued in natural circulation, saturated, and the flow decreased. This decreased the primary-to-secondary heat transfer and resulted in a heating up of the liquid exiting the core. It saturated, and as the broken loop was about to stall, voiding in the reactor vessel forced more liquid over the broken-loop U-bend, giving renewed flow. Eventually the U-bend voided fully and flow through the broken loop ceased. The final loss of natural circulation through the broken loop occurred several minutes earlier for this case than for the proposed nominal case because of the higher leak flow calculated for this test.

The lower SG-secondary refill rate gave continued AFW flow after both loops stalled. In the nominal case the refill had ended before the broken-loop stalled. As a consequence, this case had a greater depressurization rate after the loops stalled than did the nominal case. The primary pressure is lower for this case than for the nominal case after about 2000 s. After SG-secondary refill was completed at about 2800 s, the rate of depressurization slowed considerably.

The system slowly depressurized from the time the AFW ended at about 2800 s until about 4600 s, when the set point for the intact-loop SG secondary depressurization control declined to the intact-loop SG secondary pressure. At that time, steaming and AFW to the intact-loop SG secondary resulted in a strong feed-cycle BCM event, and a corresponding sharp increase in the primary depressurization rate. This increased the boiloff and level depression in the broken-loop SG primary so that it dropped below the level of the secondary side pool, giving pool BCM heat transfer starting at about 4700 s. This caused the secondary

pressure in the broken-loop SG to increase until it reached the set point pressure for controlled depressurization at about 5200 s.

Refill started at about 4700 s (Fig. 11), when the more rapid depressurization caused two-phase flow out the break. HPI flow exceeded break flow for the remainder of the calculation, although the two were approximately balanced. This condition is expected to continue, with HPI flow gradually increasing and break flow gradually decreasing.

Test 320604. Test 320604 was identical to the proposed nominal test except that the HPI capacity was roughly one-half of full HPI flow. With the lower HPI flow rate, the primary pressure (Fig. 12) and vessel inventory (Fig. 13) decreased more rapidly than in the nominal case. The intact-loop hot leg saturated at about 80 s and remained saturated for the remainder of the transient. At about 130 s, the intact-loop U-bend was fully voided; natural circulation flow through the SG primary ended about 5 s later (Fig. 14). This effectively decoupled the intact A-loop SG as a heat sink. The broken loop saturated briefly (for about 20 s) starting at 100 s; until 580 s it saturated intermittently. After that time it remained saturated with complete voiding in the U-bend occurring at 610 s and complete loss of natural circulation flow occurring about 3 s later (Fig. 14). This was slightly more than half the time for the nominal case to lose all natural circulation through the hot legs.

Following reactor trip at 45 s, the steam generator control system received a signal to fill the secondaries to the 9.63 m (95%) level. The secondary side collapsed liquid levels of the intact-loop and broken-loop SGs reached this level at about 500 and 540 s, respectively. During the refilling of the secondaries by the AFW, the secondary pressures were reduced (Fig. 12). In the intact loop, the secondary pressure remained below the ATOG set point pressure resulting in termination of steam flow by the control system. Therefore, with the exception of a small flow as the control system settled in on the level setpoint, there was no supply of AFW to the intact loop secondary after 500 s until the ATOG setpoint decreased to the intact loop steam generator pressure at 7000 s (Fig. 12). At this time steam flow was reestablished in the intact loop steam generator and AFW was then activated in the intact loop to control the steam generator level. The AFW startup at 7000 s caused a strong feed cycle BCM since the liquid level in the primary side of the intact-loop SG tubes was well below the AFW elevation this time.

In the broken loop, the ATOG-based set point pressure was recovered shortly after the SG was refilled at 540 s, since there was natural circulation in the broken loop at this time (Fig. 14). Afterward, the broken-loop SG pressure was controlled to the decreasing ATOG set point by a positive steam flow and the secondary level was maintained by a positive AFW flow. At about 1300 s, the level inside the tubes in the broken-loop SG decreased below the elevation of the AFW. From this time until 7000 s, a weak feed-cycle BCM was calculated to occur in the broken loop, which rejected some of the decay heat from the primary system. During the 540–7000 s interval, the control system for the ATOG-based pressure control alternately operated in the constant pressure control mode and in the 100°F/hr cool-down mode, depending on the core-exit temperature and the SG secondary pressures. The ATOG-based pressure was generally calculated as the saturation pressure corresponding to a saturation temperature 50°F below the core-exit temperature.

From break initiation to about 2700 s, the break discharge flow exceeded the HPI flow and the primary system inventory was being depleted. Although there were earlier periods of

two-phase flow at the break, beginning at 2700 s, periods of single-phase vapor flow out the break were predicted. This reduced the break discharge flow to approximately the HPI flow and the primary system inventory was then stabilized until the intact-loop feed-cycle BCM at 7000 s. At this time, the primary pressure was reduced by heat transfer to the intact-loop secondary and the leak flow was further reduced to a value below the HPI flow. After the start of refill at 7000 s, the primary system inventory gradually increased. The reactor vessel collapsed liquid level (Fig. 13) was calculated to remain at or above the hot-leg nozzle elevation for the duration of Test 320604.

The same phenomena and overall system behavior were calculated for the reduced HPI Test 320604 as for the specified nominal Test 310000. The main effect of the reduced HPI flow was to change the timing of major events. The interruption of natural circulation was calculated to occur earlier in the transient with the reduced HPI flow since the hot legs drained faster. After the interruption of natural circulation, the primary system depressurized more slowly with reduced HPI flow because the feed-and-bleed cooling of the HPI-leak flow was reduced. The minimum primary-system inventory was not strongly affected by the reduced HPI flow in Test 320604 because the leak flow was also reduced as a result of higher void fractions calculated in the cold leg upstream of the leak.

Test 330201. This transient calculation was initiated by the termination of all AFW to the SG secondaries. There were two immediate consequences of AFW termination. First, the heat removal capacity of the steam generators was reduced. Because the primary is liquid solid (full of liquid,) the excess core decay energy was deposited in the primary coolant and the temperature began to rise. The resultant coolant expansion in the solid system caused the primary pressure to rise (Fig. 15). Second, with the cessation of AFW, the SG thermal centers moved to a lower level in the SGs. With the reduction in driving head, the primary loop natural-circulation flows decreased markedly. The natural-circulation flows in the primary loops subsequently recovered as the primary heated up; the first recovery occurred in the intact loop followed by recovery of the broken loop (Fig. 16). However, the loop flows went through several long-period cycles and remained out of phase until natural circulation was terminated by voiding at the top of the hot-leg U-bends.

By 570 s, the primary pressure had increased to the PORV set point value of 16.2 MPa (2350 psi). The PORV opened at its set point and was locked open for the remainder of the transient; this constituted the bleed action in the feed-and-bleed transient. At the same time, the cold-leg HPI flow was initiated; this constituted the feed action in the feed-and-bleed transient. The core power decay was then initiated after a delay of 10 s. After the PORV was opened, the primary pressure rapidly decreased until the fluid in the upper plenum, upper head, and hot legs reached saturation. Shortly after, the top of the intact-loop U-tube voided and intact-loop natural circulation was lost. This also represented the effective loss of the intact-loop SG as a heat sink. As a consequence, the primary system began to repressurize at about 750 s and the boiloff rate in the intact-loop SG was reduced. The boiloff of the liquid in the intact-loop SG secondary was completed by about 1100 s.

By 890 s, the pressurizer was full of liquid and fluid passing through the PORV changed from a two-phase mixture to liquid. Consequently, less energy was relieved from the primary. Core decay energy was again deposited in the primary coolant and caused the core outlet

liquid temperature to increase. Because only the broken loop remained liquid full, the natural-circulation flow through the broken loop began to increase rapidly. Steam production in the broken-loop SG also increased; sufficient energy was removed that the primary repressurization was briefly terminated from 920 s to 950 s when the broken-loop SG was boiled dry. After 950 s the primary system continued to repressurize until the broken-loop U-bend voided at 1225 s, terminating natural circulation in the broken loop. Shortly afterward, two-phase flow through the PORV was re-established and the primary system repressurization was terminated. The energy relief through the PORV and the core decay heat approached an approximate balance and a slow decline of pressure at the rate of 700 Pa/s (0.102 psi/s) was then established for the remainder of the calculated transient. By 3070 s the primary pressure had reduced to 11.5 MPa (1668 psi).

Test 330302. The phenomena in this calculation were quite similar to those in Test 330201. The transient from initiation to opening the PORV at 568.5 s was identical to that for Test 330201. For this transient, the cold-leg HPI flow initiation was delayed 1200 s until 1787.5.

From the time the PORV opened until HPI actuation, the MIST facility experienced primary-system inventory depletion. Inventory was lost from both the vessel and the primary loops. However, for the period between 1375 to 1640 s, the vessel inventory remained nearly constant; liquid drainage from the cold legs and the reactor-coolant pumps into the downcomer replenished vessel inventory. At 1640 s, the inventory of the cold legs and reactor-coolant pumps is depleted and the vessel inventory begins to decline rapidly as shown in Fig. 17. The collapsed liquid level decreased to the hot-leg nozzles; vapor flow into the hot legs then retarded further drainage of liquid into the vessel upper plenum. Vessel inventory depletion continued until HPI initiation. The HPI flow was sufficient to immediately begin refilling the vessel. Once the vessel mixture level reached the hot-leg nozzles, vapor flow into the hot legs was terminated. Vessel-downcomer natural circulation through the RVVVs was then re-established, and energy relief through the PORV and the core decay heat approached an approximate balance. The primary then settled into a nearly constant rate of depressurization and cooldown until the end of the calculated transient at 2480 s. The calculation was terminated when it was evident that the refilling process would continue without interruption.

CONCLUSIONS AND RECOMMENDATIONS

Results of the five pretest calculations indicate that the MIST facility can be expected to exhibit a characteristic post-SB LOCA behavior under a wide variety of imposed boundary conditions. The initial loop behavior was common to all five of the calculations. After leak initiation or PORV opening, this behavior included the interruption of natural circulation in the intact loop, followed by a sharp reduction in broken-loop natural circulation flow and the start of primary system repressurization. It also included a subsequent period of spillover circulation in the broken loop sufficient to stop the repressurization. After this sequence of events, natural circulation was completely terminated in both loops and the calculated system response depended on the control procedures specified for the test. Strong system interactions and coupling were observed in each of the pretest calculations. For example, during liquid-continuous primary natural circulation, the primary loops experienced several long-period flow oscillations. The presence of the pressurizer in the intact loop was the trigger that initiated the differing thermal-hydraulic behaviors of the intact and broken loops.

The pretest calculations were performed through the blowdown phase of the transient and each calculation was terminated near the beginning of refill when the HPI flow exceeded the leak flow. The MIST scaling and operation atypicalities generally tend to extend the times required for various events to occur and to exaggerate the asymmetries of the facility; however, the overall trends of the calculations were not affected by the scaling atypicalities.

Results of the pretest calculations indicated that the MIST facility safety limits would not be approached in the five tests considered. First, core uncovery will not occur during any of the tests examined. The lowest vessel liquid levels were predicted for Test 330302, feed-and-bleed cooling with HPI delayed 20 minutes after PORV actuation. Second, PORV capacity is sufficient to maintain the primary-system pressure below the relief valve set points during the feed-and-bleed tests.

The only observed deficiencies in the code involved the AFW wetting model and the ability to represent cross flows in the secondary. The AFW wetting problem involves the combination of the specified degree of tube wetting on the secondary and the heat-transfer correlations that are invoked; it results in the calculated thermal center of the steam generator being too low and causes the calculated primary natural circulation flow at the beginning of the transients to be low. We do not anticipate this to be a problem in plant calculations except possibly during the early stages of some transients when the secondary filling by AFW occurs after the primary coolant pumps have coasted down and flow is driven by natural circulation. The other deficiency involves the ability of the parallel channel secondary used in these analyses to represent the necessary cross flows; this modeling capability should be improved in TRAC-PF1/MOD2, which will permit one to use the VESSEL component to model steam-generator secondaries.

The results of the pretest calculations will be used as a basis for subsequent assessment of the TRAC-PF1/MOD1 code, which will ultimately be used to extrapolate data from the MIST facility to full-scale plant behavior.

REFERENCES

1. Safety Code Development Group, "TRAC-PF1/MOD1: An Advanced Best-Estimate Computer Program for Pressurized Water Reactor Thermal-Hydraulic Analysis," Los Alamos National Laboratory report LA-10157-MS (NUREG/CR-3858) (July 1986).

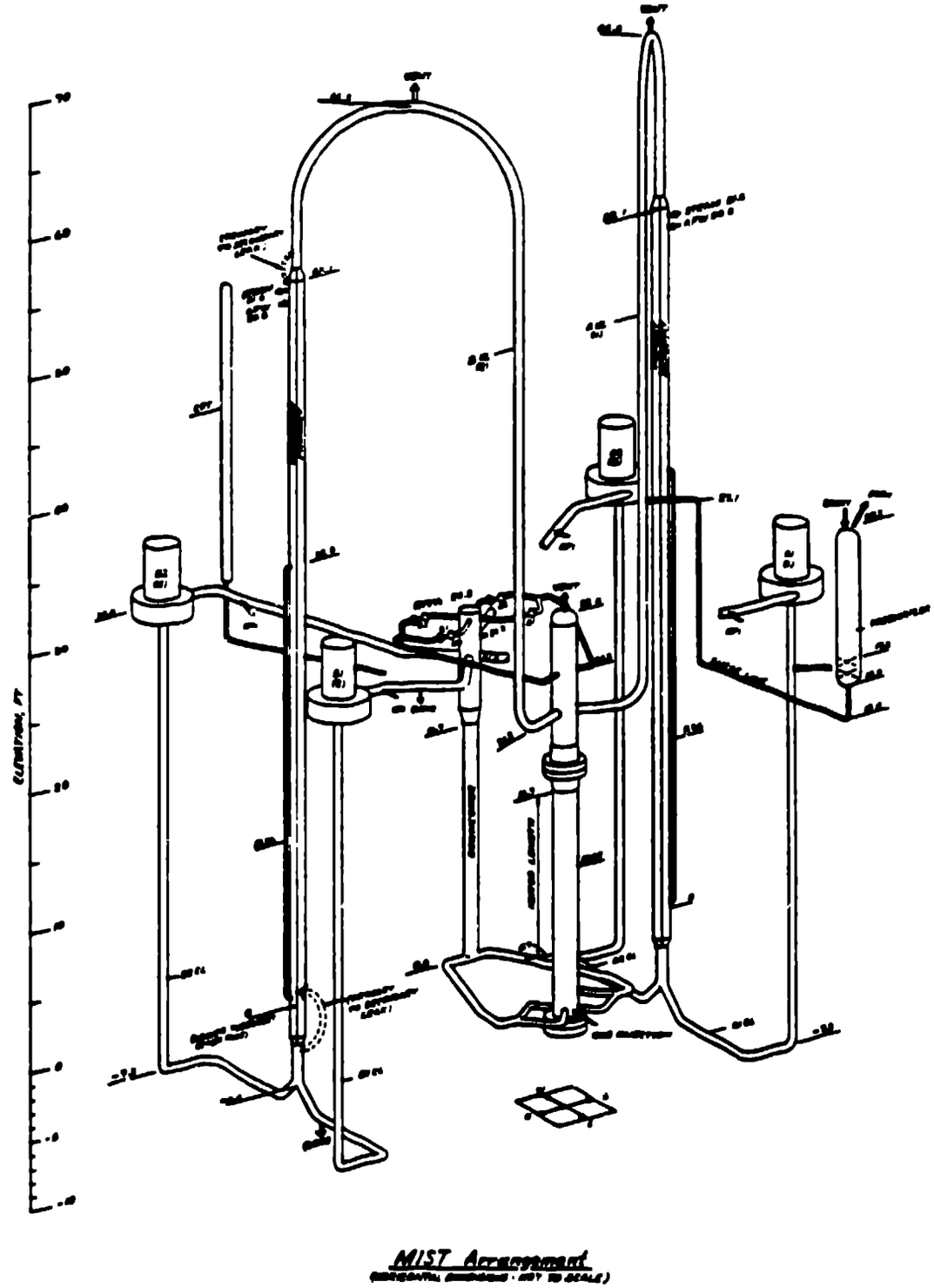

Fig. 1.
MIST facility.

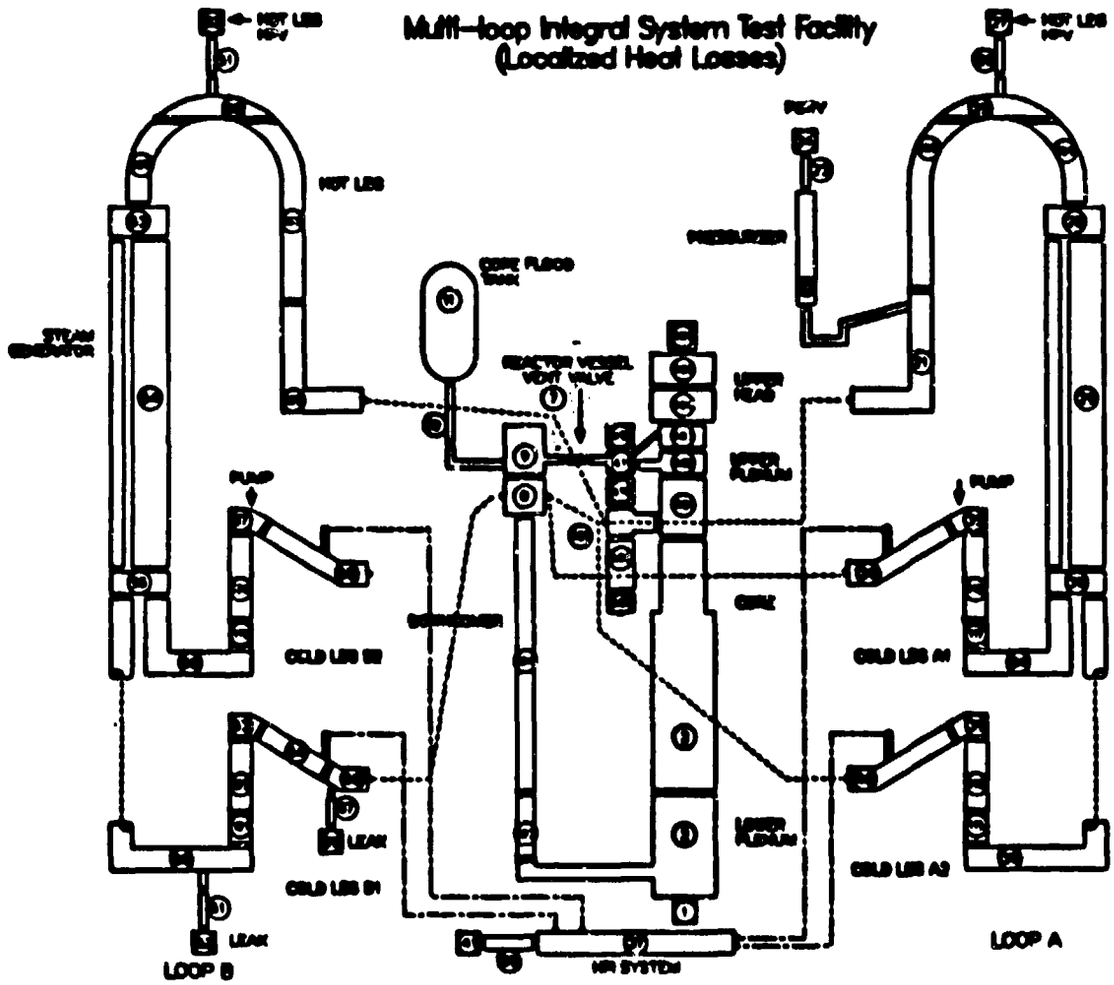

Fig. 2.
TRAC component noding schematic.

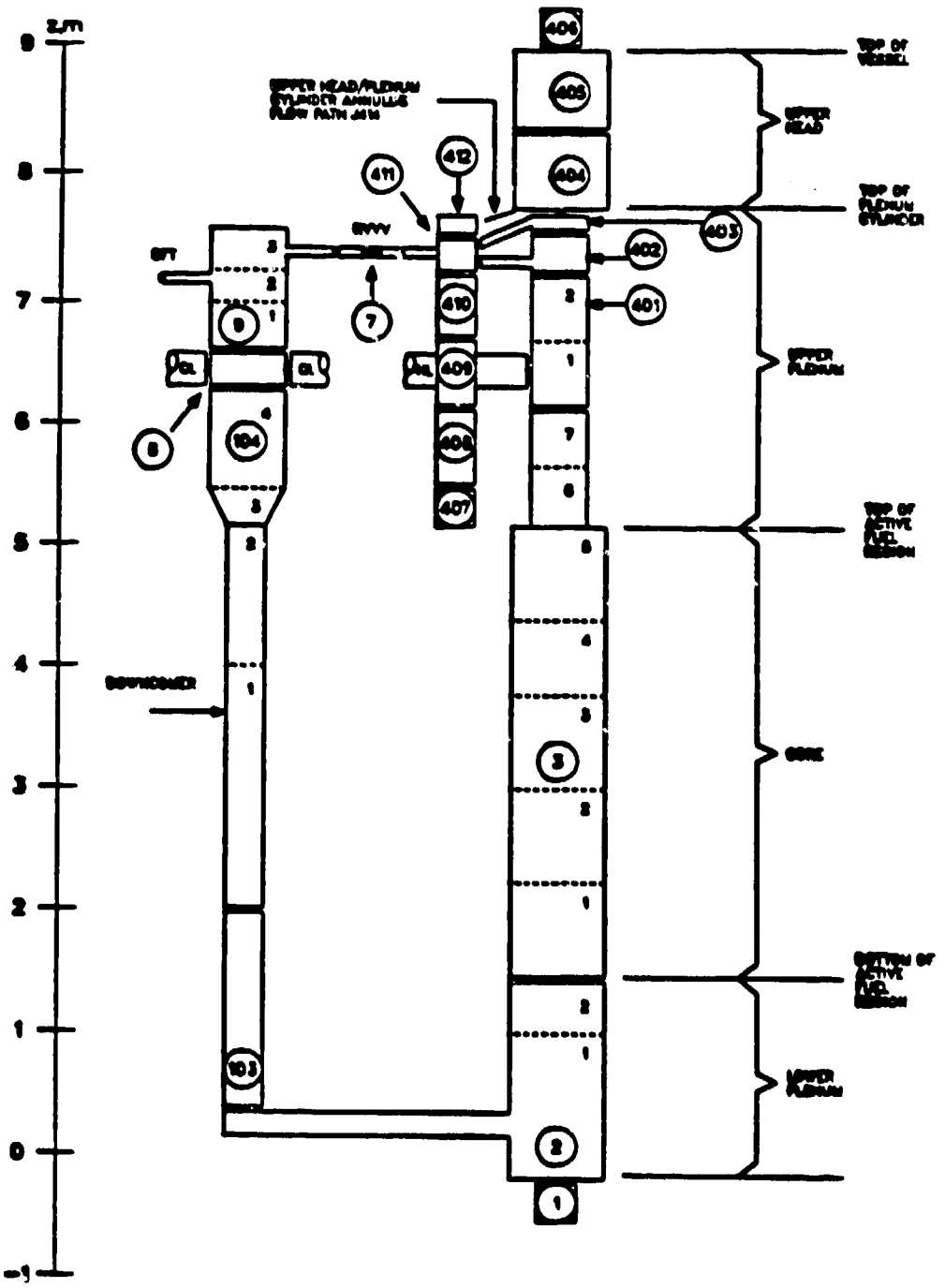

Fig. 3.
TRAC reactor vessel noding schematic.

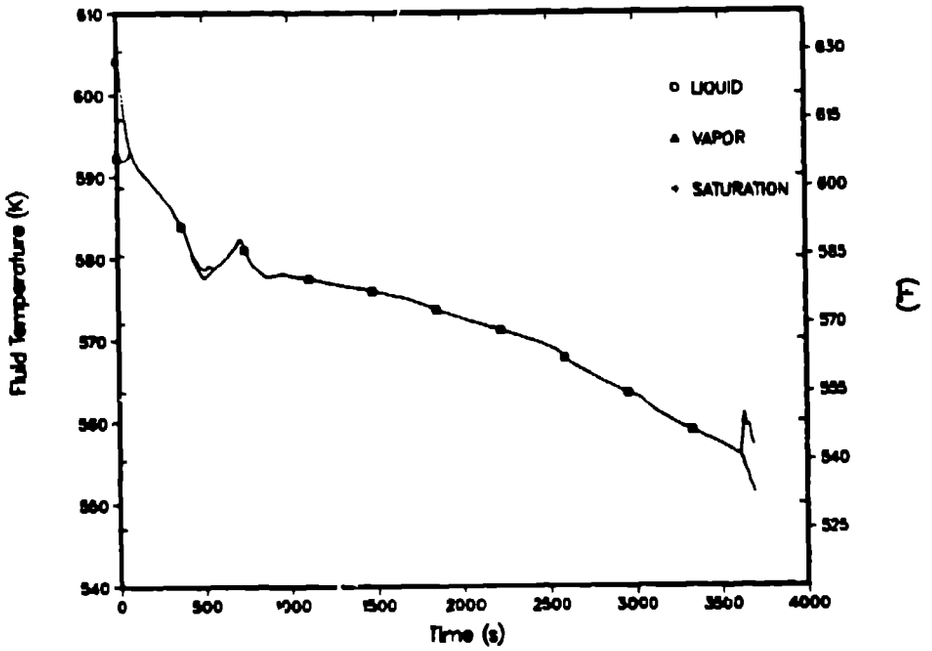

Fig. 4.
TRAC calculation for Test 310000, temperatures in intact-loop hot-leg U bend.

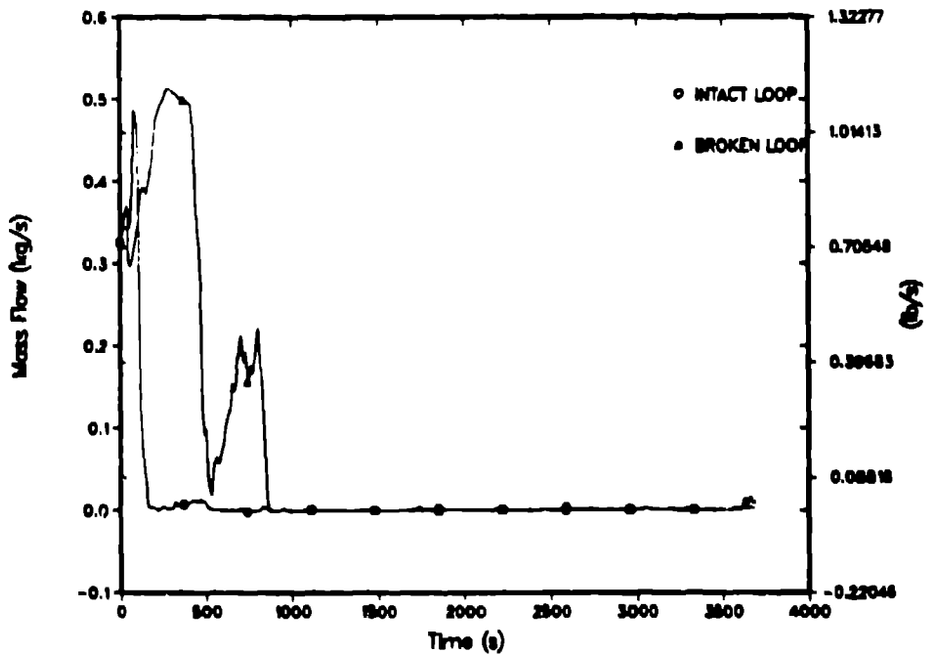

Fig. 5.
TRAC calculation for Test 310000, hot-leg U-bend mass flows.

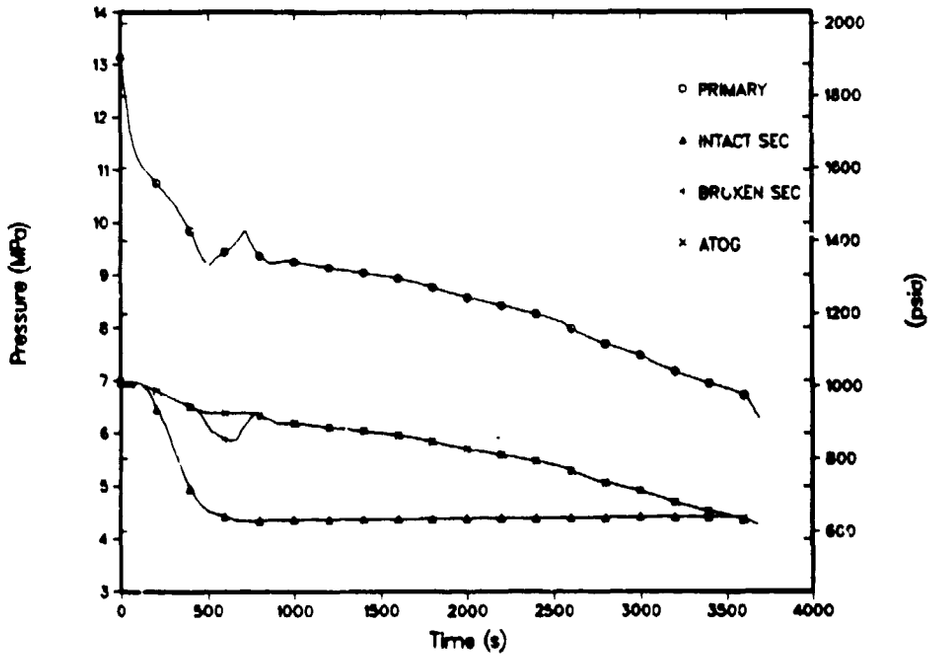

Fig. 6.
TRAC calculation for Test 310000, primary and secondary system pressures.

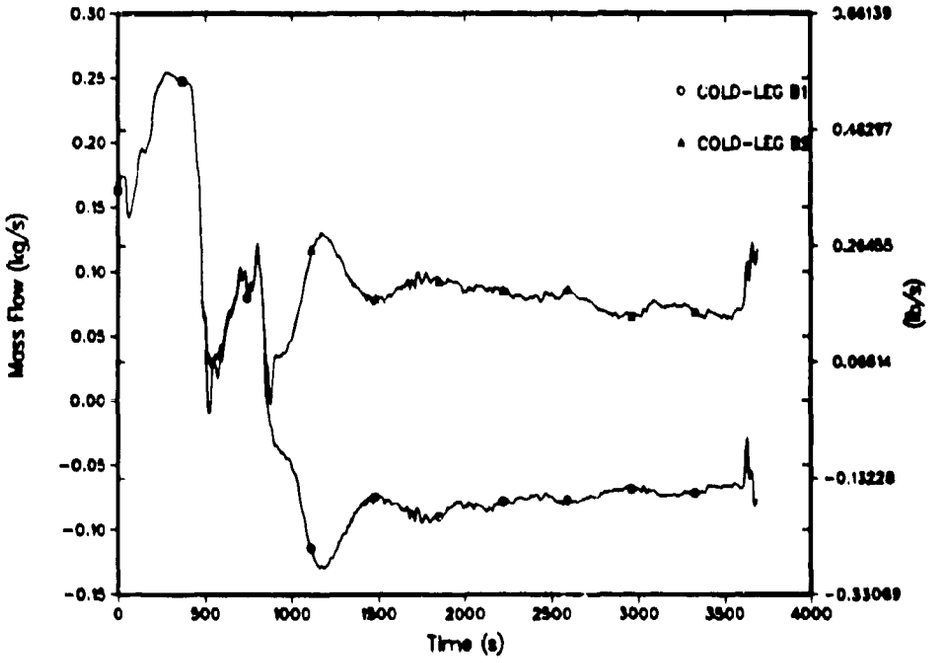

Fig. 7.
TRAC calculation for Test 310000, broken-loop cold-leg pump-suction mass flows.

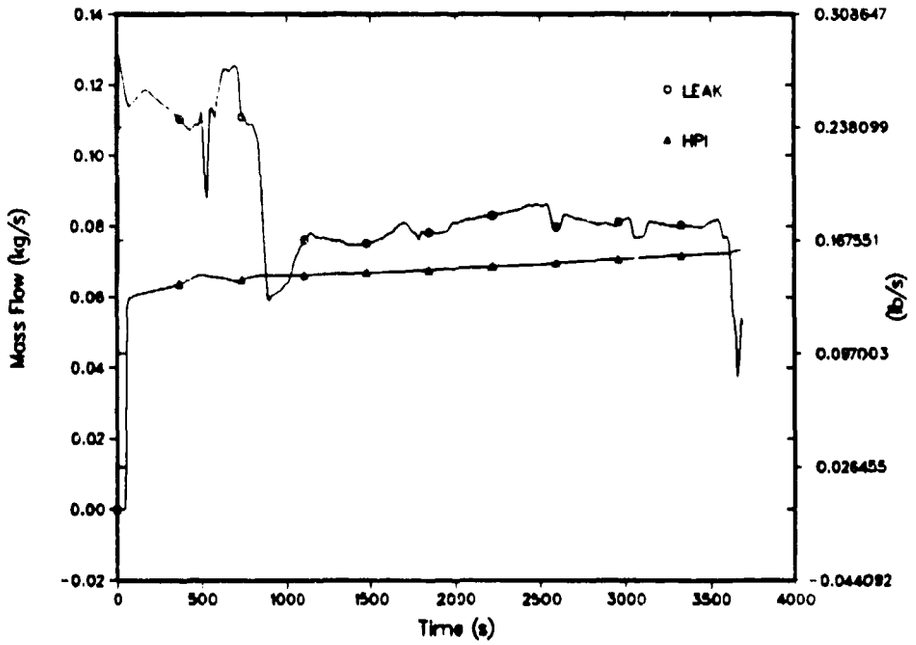

Fig. 8.
TRAC calculation for Test 310000, cold-leg leak and HPI flows.

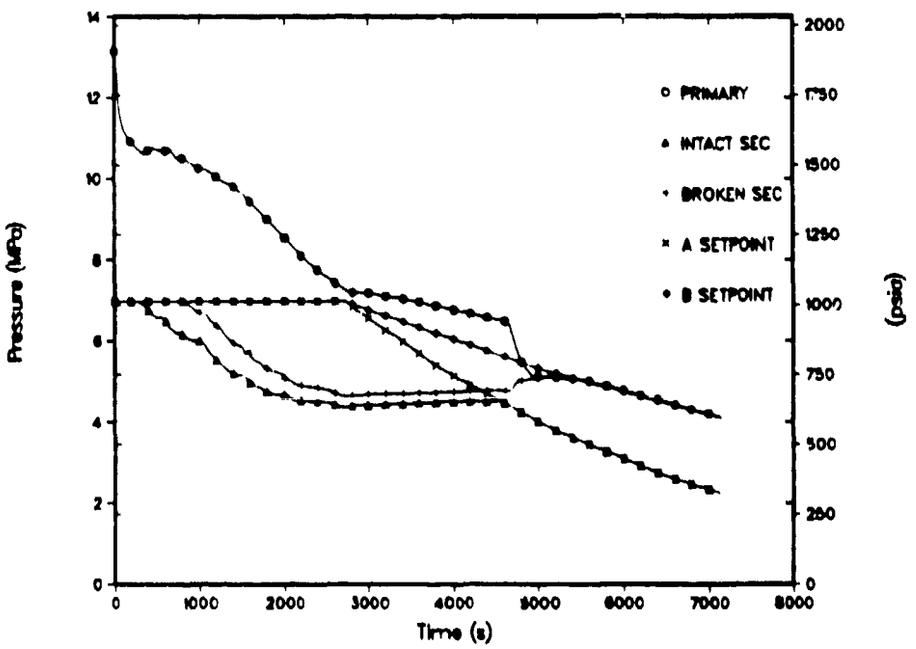

Fig. 9.
TRAC calculation for Test 310503, primary and secondary system pressures.

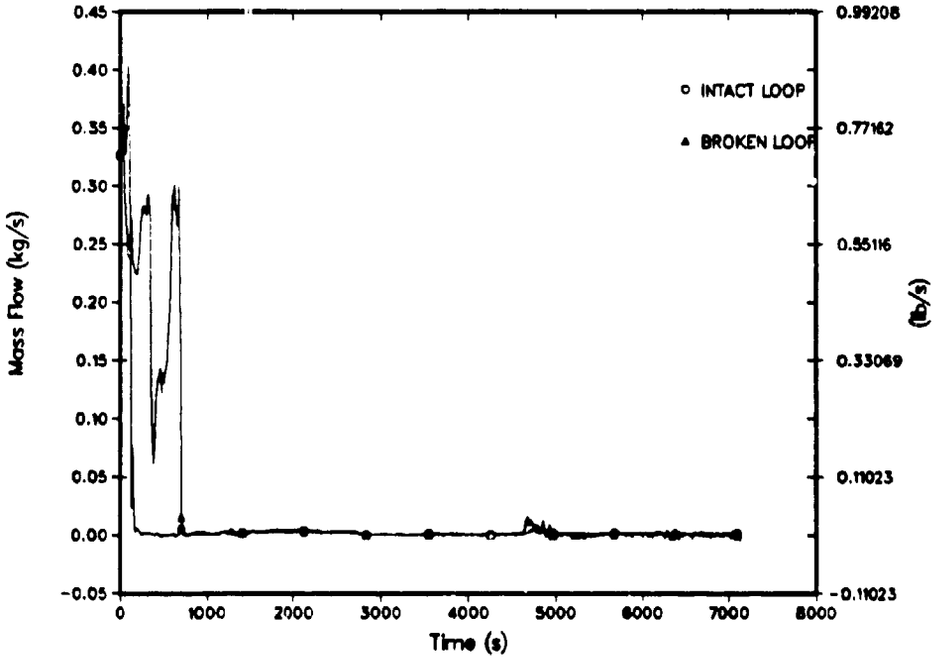

Fig. 10.
TRAC calculation for Test 310503, hot-leg U-bend mass flows.

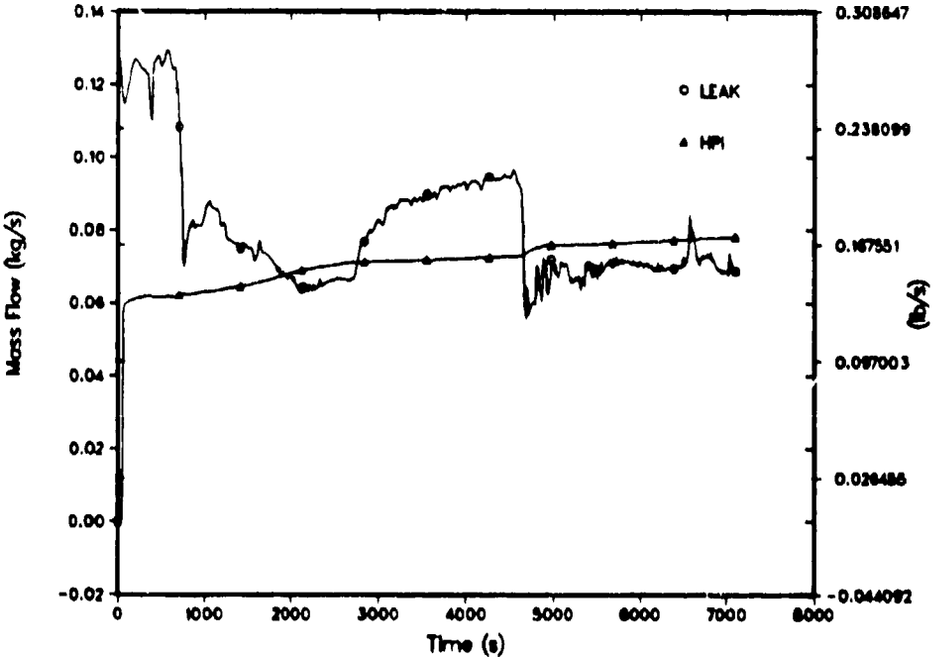

Fig. 11.
TRAC calculation for Test 310503, cold-leg leak and HPI flows.

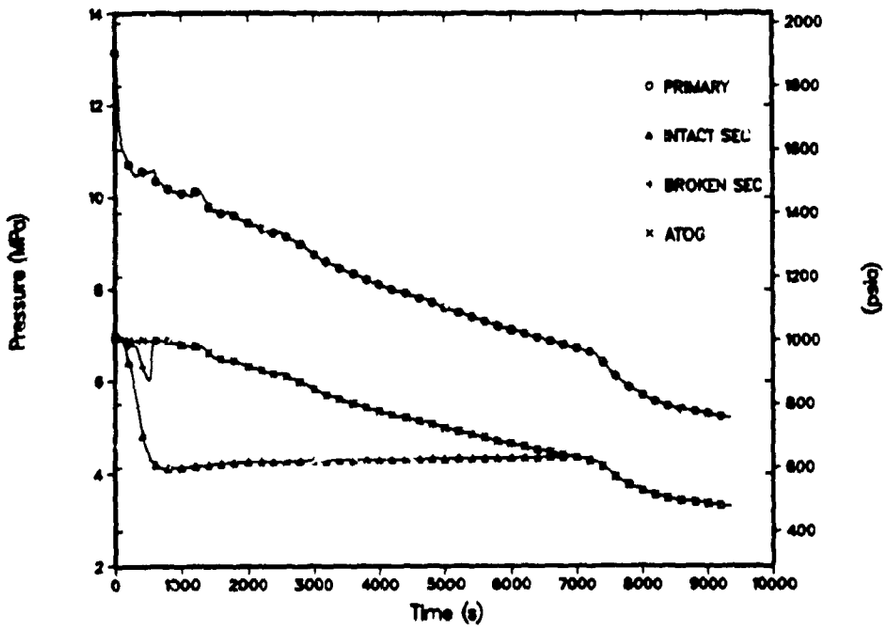

Fig. 12.
TRAC calculation for Test 320604, primary and secondary system pressures.

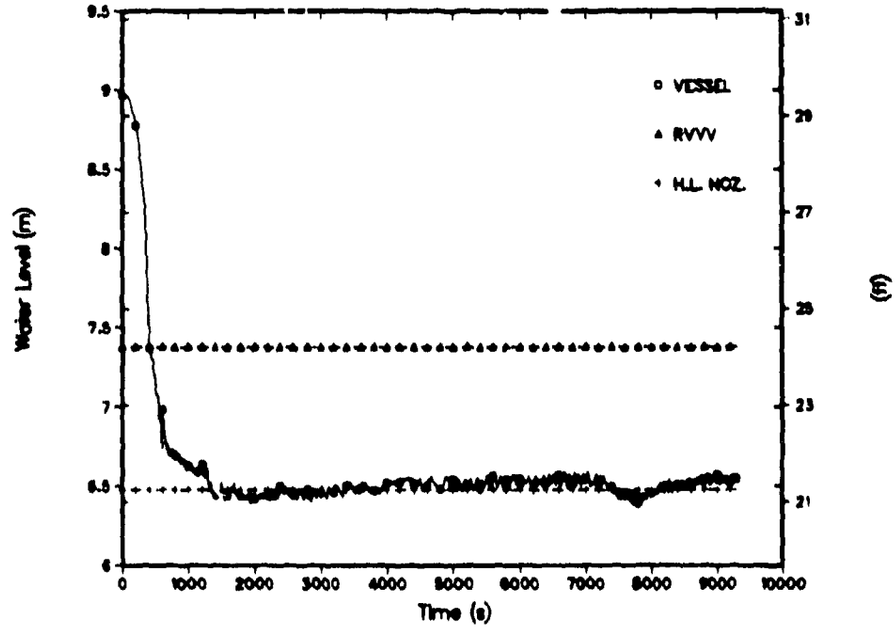

Fig. 13.
TRAC calculation for Test 320604, reactor vessel collapsed liquid level.

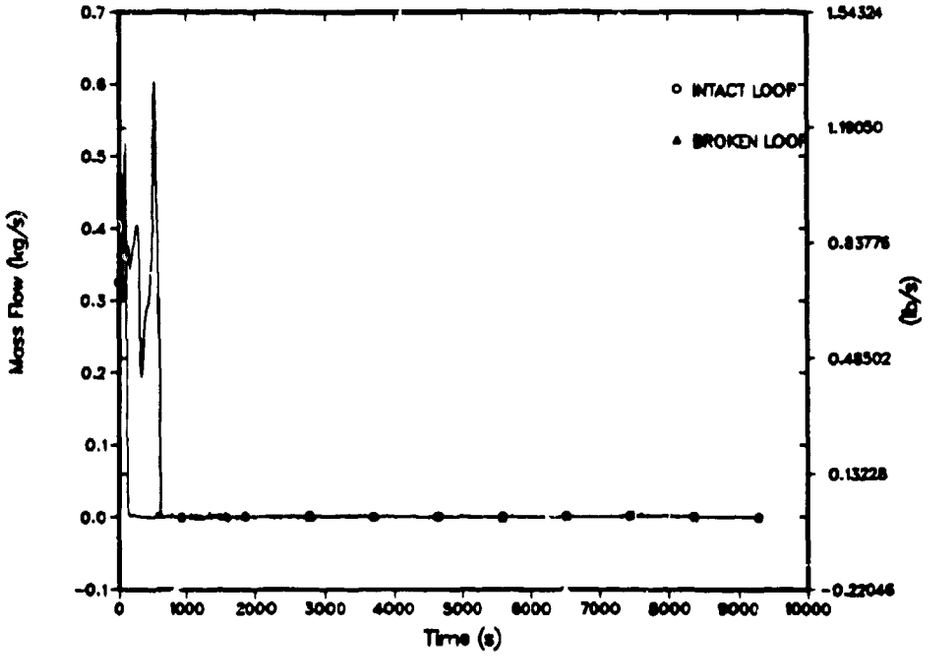

Fig. 14.
TRAC calculation for Test 320604, hot-leg U-bend mass flows.

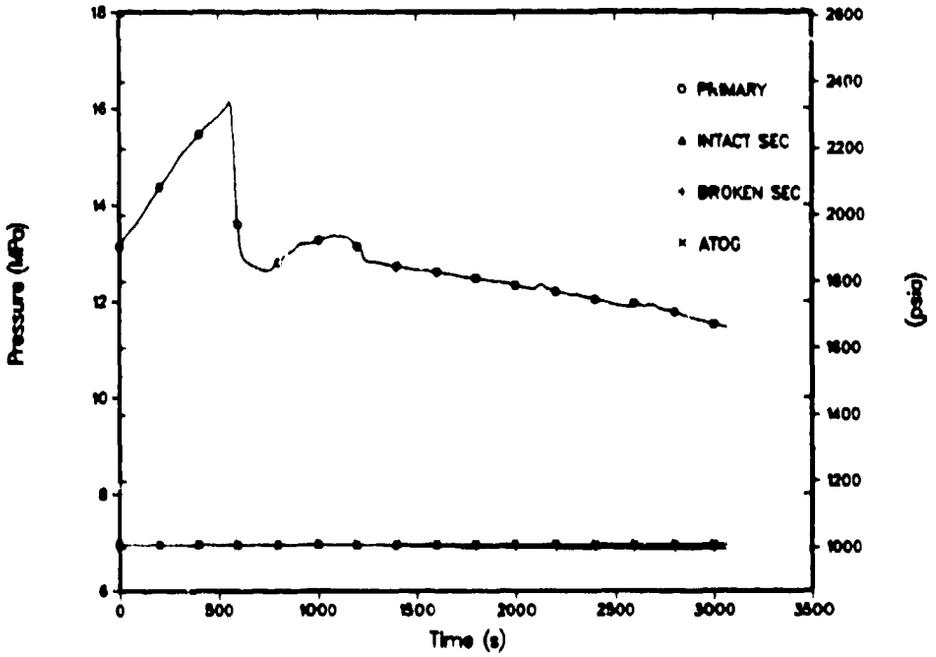

Fig. 15.
TRAC calculation for Test 330201, primary and secondary system pressures.

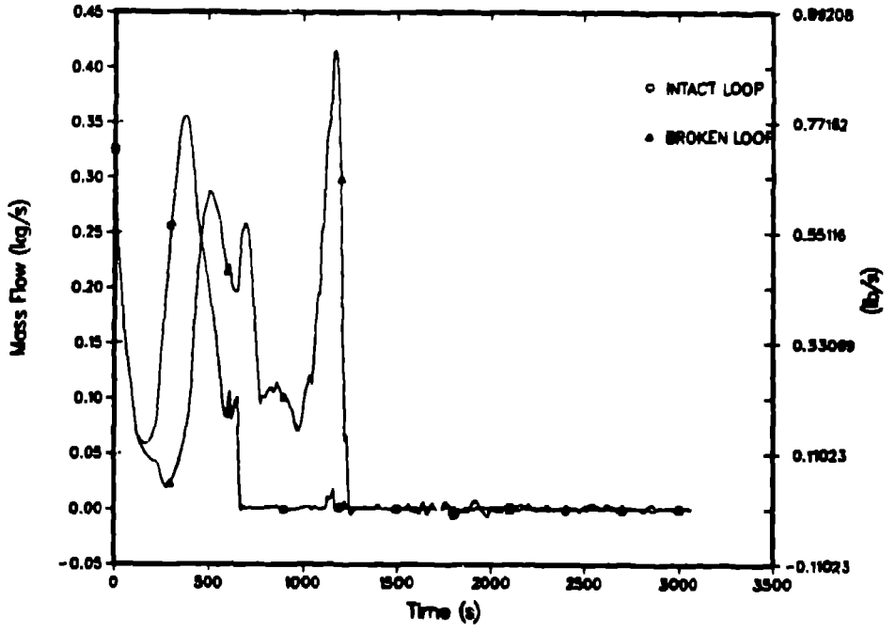

Fig. 16.
TRAC calculation for Test 330201, hot-leg U-bend mass flows.

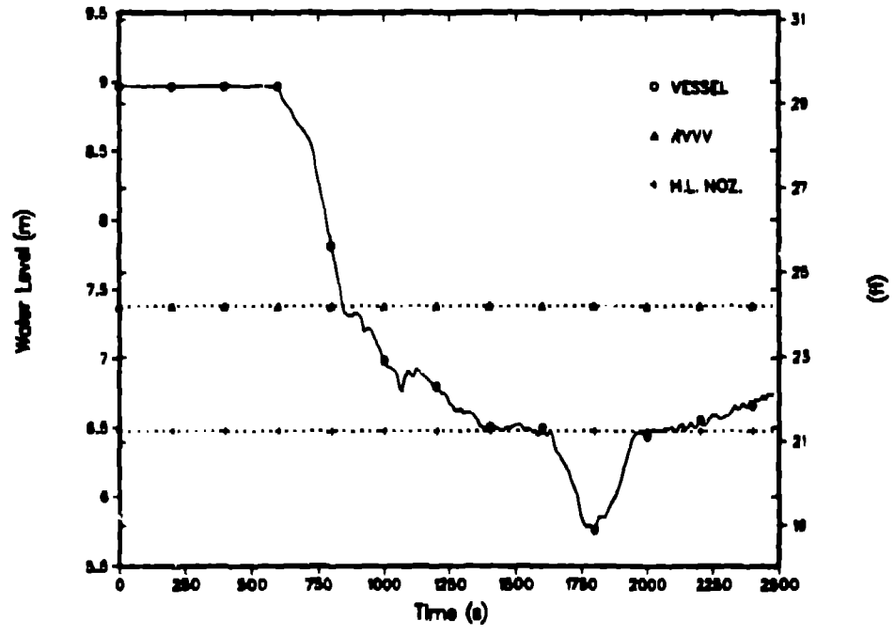

Fig. 17.
TRAC calculation for Test 330302, reactor vessel collapsed liquid levels.